

Polarization-dependent asymmetric light scattering by silicon nanopylramids and their multipoles resonances

Cite as: J. Appl. Phys. **125**, 173108 (2019); <https://doi.org/10.1063/1.5094162>

Submitted: 27 February 2019 . Accepted: 14 April 2019 . Published Online: 03 May 2019

Pavel D. Terekhov , Andrey B. Evlyukhin , Alexander S. Shalin, and Alina Karabchevsky 



View Online



Export Citation



CrossMark

ARTICLES YOU MAY BE INTERESTED IN

[Experimental demonstration of spectrally broadband Huygens sources using low-index spheres](#)

APL Photonics **4**, 020802 (2019); <https://doi.org/10.1063/1.5080980>

[Analogue of the Kerker effect for localized modes of discrete high-index dielectric nanowaveguides](#)

Journal of Applied Physics **125**, 123104 (2019); <https://doi.org/10.1063/1.5087248>

Applied Physics Reviews
Now accepting original research

2017 Journal
Impact Factor:
12.894

Polarization-dependent asymmetric light scattering by silicon nanopyramids and their multipoles resonances

Cite as: J. Appl. Phys. **125**, 173108 (2019); doi: [10.1063/1.5094162](https://doi.org/10.1063/1.5094162)

Submitted: 27 February 2019 · Accepted: 14 April 2019 ·

Published Online: 3 May 2019



Pavel D. Terekhov,^{1,2,3,4,a)} Andrey B. Evlyukhin,^{2,5,6} Alexander S. Shalin,^{2,7} and Alina Karabchevsky^{1,3,4,b)}

AFFILIATIONS

¹Electrooptics and Photonics Engineering Department, Ben-Gurion University, Beer-Sheva 8410501, Israel

²ITMO University, 49 Kronversky Ave., 197101, St. Petersburg, Russia

³Ilse Katz Institute for Nanoscale Science & Technology, Ben-Gurion University, Beer-Sheva 8410501, Israel

⁴Center for Quantum Information Science and Technology, Ben-Gurion University, Beer-Sheva 8410501, Israel

⁵Institute of Quantum Optics, Leibniz Universität Hannover, 30167 Hannover, Germany

⁶Moscow Institute of Physics and Technology, 9 Institutsky Lane, Dolgoprudny 141700, Russia

⁷Faculty of Physics and High Technology Engineering, Ulyanovsk State University, Ulyanovsk 432017, Russia

Note: This paper is part of the Special Topic on Dielectric Nanoresonators and Metamaterials.

^{a)}Electronic mail: terekhovpd@gmail.com

^{b)}Electronic mail: alinak@bgu.ac.il

ABSTRACT

For a long time, light manipulation at the nanoscale has been provided primarily with plasmonic materials. However, recent works show that the light can be controlled with dielectric particles. Here, we exploit the asymmetric shape of silicon nanopyramids to control the far-field scattering pattern and the electric field concentration inside the particles by simply changing the incident light polarization. This effect is considered both in air and lossless optical medium. For an explanation of the demonstrated features, we apply the multipole analysis of the scattering cross sections. We show that the electric and magnetic quadrupole resonances can be switched between them by changing the incident wave polarization providing changes of the scattering diagrams. We also show that the polarization control of the scattering properties of pyramidal nanoparticles strongly depends on the refractive index of the surrounding medium. The obtained results can be used for the development of optical antennas, switchers, and polarization filters composed of silicon materials.

Published under license by AIP Publishing. <https://doi.org/10.1063/1.5094162>

I. INTRODUCTION

Light-matter interaction of dielectric or plasmonic structures is extensively studied.^{1–5} Conventional optical devices, such as mirrors and lenses direct, focus, or diverge the light. However, this light manipulation is limited by the diffraction. At the subdiffraction limit regime the light manipulation can be also achieved with subwavelength structures.^{1,2,6,7} Compared to plasmonic nanostructures, dielectric nanostructures having simple particle geometries provide both electric and magnetic responses^{3,4,8–10} and decrease Joule losses, which is naturally present in metals.^{4,11}

The particular case of scattering by spherical nanoparticles can be studied using the Mie theory.¹² The analysis based on the

Mie theory provides important information about the origins of the scattering phenomena. However, spherical particles limit a study due to a fixed shape and aspect ratio. Nonspherical nanoparticles can be studied, for example, using the Cartesian multipole decomposition semianalytical approach. Recently, it was shown that particles' geometry, aspect ratio, and material dispersion affect the light-matter interaction leading to a change in particles' optical properties.^{13,14} Mutual interaction between multipole moments resulting in overlapping their resonances can be explored for engineering nanoantennas,^{15–18} sensors,^{19,20} optical filters,²¹ energy harvesting devices,^{22,23} and cloaking.^{24,25} Anapole physics is another area where multipole interaction is a keynote.^{26–28} It is

worth noting that multipole decomposition approach can also be applied for studies in the terahertz frequency range²⁹ and even for macroscopic objects like the Great Pyramid.³⁰

Silicon is one of the highly demanded materials in modern dielectric nanophotonics due to its large refractive index and low absorption at near-infrared frequencies.^{31–33} However, its absorption increases in the visible spectral range.³⁴ Nevertheless, for relatively small particles comparing to an incident wavelength, the absorption can be neglected.

Here, we implement the Cartesian multipole decomposition approach^{35,36} to study pyramidal silicon nanoparticles and exploit their asymmetry to control light scattering at the nanoscale. The lateral faces of the explored pyramids are illuminated with orthogonally polarized light (Fig. 1). We expand our research conducted in Ref. 13 to study lateral illumination of a silicon nanopyramid. It is important to study the influence of asymmetric shape on light scattering by nanoparticles. Comparing to spherical nanoparticles,³⁷ which only have one geometrical degree of freedom, complex particle shapes provide much more possibilities to tune a spectral response. Particularly, there is no dependence on polarization conditions in the case of spherical particles. In addition, far-field diagrams of spherical nanoparticles are always symmetric, and the spectral order of multipole moments is rigidly fixed. For silicon pyramids, we show that the incident wave polarization switches the resonant excitation of either electric quadrupole or magnetic quadrupole moments.

II. THEORETICAL BACKGROUND

Here, we consider the optical system including a single silicon nanopyramid suspended in air and in a lossless medium with a refractive index of $n_{env} = 1.31$. Figure 1 shows the schematics of the nanopyramid with base edge of $D = 250$ nm and height of $H = 250$ nm, made of polycrystalline silicon.³⁴ Incident wave illuminates the lateral facet of the pyramid. Note that the k -vector of

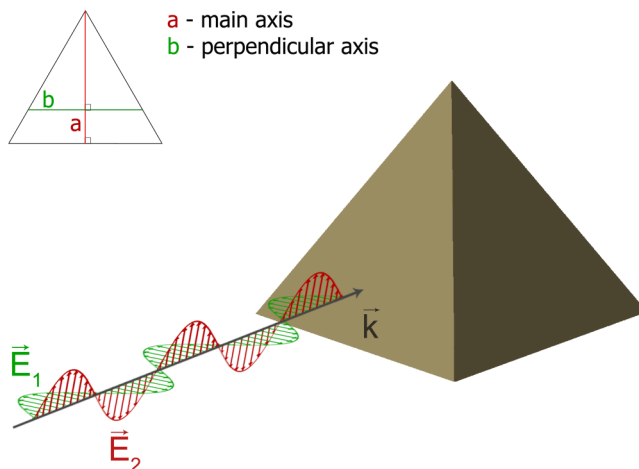


FIG. 1. Rendered silicon nanopyramid. The pyramid lateral facet is illuminated by the plane wave of orthogonally polarized waves.

the incident wave is parallel to the pyramid base and normal to pyramid's main axis, as shown in Fig. 1. To study the influence of the incident wave polarization on the scattering effect, we compare the electric field polarization oriented (1) along the axis through the vertex and (2) along the base of the nanopyramid.

To analyze the considered system, we use the semianalytical multipole decomposition approach reported in Ref. 35. This approach is based on the multipole expansions frequently used in the electrodynamic theory.^{35,36,38} Here, we use the expressions of the multipole moments beyond the long-wavelength approximation defined in Ref. 36. Note that for scatterers located in a medium, the wavenumber, substituted in the expressions for multipoles,³⁶ should be multiplied by the refractive index of this medium. We validated that the considered set of multipole moments is sufficient for the proper description of the system we study. The full electric field in the system is numerically calculated with the finite element method (FEM) implemented in COMSOL Multiphysics commercial package.^{39,40} The calculated electric field is used for obtaining the multipole moments and their contributions to the scattering cross sections.^{35,36,38}

The scattering cross section of a particle in a homogenous host medium can be presented as (see Ref. 35 for details)

$$C_{sca} \simeq \frac{k_0^4}{6\pi\epsilon_0^2|\mathbf{E}_{inc}|^2}|\mathbf{p}|^2 + \frac{k_0^4\epsilon_d\mu_0}{6\pi\epsilon_0|\mathbf{E}_{inc}|^2}|\mathbf{m}|^2 + \frac{k_0^6\epsilon_d}{720\pi\epsilon_0^2|\mathbf{E}_{inc}|^2}|\hat{Q}|^2 + \frac{k_0^6\epsilon_d^2\mu_0}{80\pi\epsilon_0|\mathbf{E}_{inc}|^2}|\hat{M}|^2 + \frac{k_0^8\epsilon_d^2}{1890\pi\epsilon_0^2|\mathbf{E}_{inc}|^2}|\hat{O}|^2, \quad (1)$$

where \mathbf{E}_{inc} is the electric field amplitude of the incident light wave, $\epsilon_d = n_d^2$ is a relative dielectric permittivity of the surrounding medium, ϵ_0 is the vacuum electric permittivity and $v_d = c/\sqrt{\epsilon_d}$ is the light speed in the surrounding medium; k_0 and k_d are the wavenumbers in vacuum and in a surrounding medium, respectively. \mathbf{m} is a magnetic dipole moment (MD) of a particle; \mathbf{p} is a total electric dipole moment (TED); \hat{Q} , \hat{M} , and \hat{O} are electric quadrupole moment tensor (EQ), magnetic quadrupole moment tensor (MQ), and tensor of an electric octupole moment (OCT), respectively. Note that these tensors are symmetric and traceless and in tensor notation e.g., \hat{Q} is equal to $Q_{\alpha\beta}$, where the subscript indices denote components (e.g., $\alpha = x, y, z$).³⁵ The total scattering cross section is obtained through the integration of the Poynting vector over a closed surface in the far-field zone and the normalization to the incident field intensity.

III. RESULTS AND DISCUSSION

We show that due to such asymmetric shape, light scattering can be controlled with a simple switching of the incident light polarization. In order to analyze this effect, we pay attention to the second- and third-order multipoles' contributions to scattering, namely, we note the dependence of the resonant behavior of quadrupole moments on the polarization. First, we study silicon nanopyramids in air and in dielectric surrounding medium with a refractive index $n_{env} = 1.31$. Second, we consider the far-field radiation patterns for both cases and their polarization dependence.

A. Multipole decomposition in different media

In this subsection, we analyze scattering cross sections of pyramidal nanoparticles in air and in medium with $n_{env} = 1.31$. Figures 2(a) and 2(b) present the multipole decomposition of the scattering cross section spectra for two polarizations of the incident plane wave. The most interesting wavelength region is located in $500 \text{ nm} \leq \lambda \leq 600 \text{ nm}$. As one can see in Fig. 2(a), if the electric field polarization of the incident wave is directed along the main axis of a nanopyramid, noticeable resonant excitation of magnetic quadrupole moment appears in the considered region. However, if the electric field polarization directed perpendicularly to the main axis, one can note the resonant excitation of electric quadrupole moment [Fig. 2(b)].

Figures 2(c) and 2(d) show the scattering cross sections for the medium with $n_{env} = 1.31$ for the same light polarization as in Figs. 2(a) and 2(b). Here, we show that embedding the particle into the lossless medium with $n_{env} = 1.31$ allows to excite either MQ or EQ resonance at the same wavelength depending on the incident wave polarization. As can be seen, the MQ moment provides the dominant contribution for the polarization directed along the main axis, while the EQ moment provides the dominant contribution for the opposite case. Thereby, resonant excitations of quadrupole moments at $\lambda = 574 \text{ nm}$ [Figs. 2(c) and 2(d)] can be switched with each other simply by changing the polarization condition. Such a feature follows from the fact that electric multipole moment

resonances experience bigger red shift than their magnetic counterparts as n_{env} rises.⁴¹

As can be seen in Fig. 2, the sum of multipole contributions is in a good agreement with directly calculated scattering cross section. The small discrepancy between these spectra can be explained with nonresonant high-order multipole contributions, which are not taken into account in our multipole decomposition. Note that the high-order multipoles, higher than the electric octupole, have been considered in the long-wave approximation in Ref. 42. In Sec. III B, we consider far-field radiation patterns for both surroundings and study their polarization dependence.

B. Far-field radiation patterns

We note four interesting wavelengths between $\lambda = 500 \text{ nm}$ and $\lambda = 600 \text{ nm}$ to compare far-field radiation patterns and analyze multipole interaction. Figure 3 presents the far-field radiation patterns at $\lambda = 537 \text{ nm}$, $\lambda = 549 \text{ nm}$, $\lambda = 563 \text{ nm}$, and $\lambda = 576 \text{ nm}$. The coordinate system in Fig. 3 is tied to the incident wave, that is, the x axis of the Cartesian system is directed along the electric field polarization, and the y axis is directed along the magnetic field polarization. In turn, the z axis is directed along the k -vector of the incident wave. As depicted in the top of Fig. 3, the left column in Fig. 3 corresponds to the electric field polarization along the main axis, and the right column corresponds to the

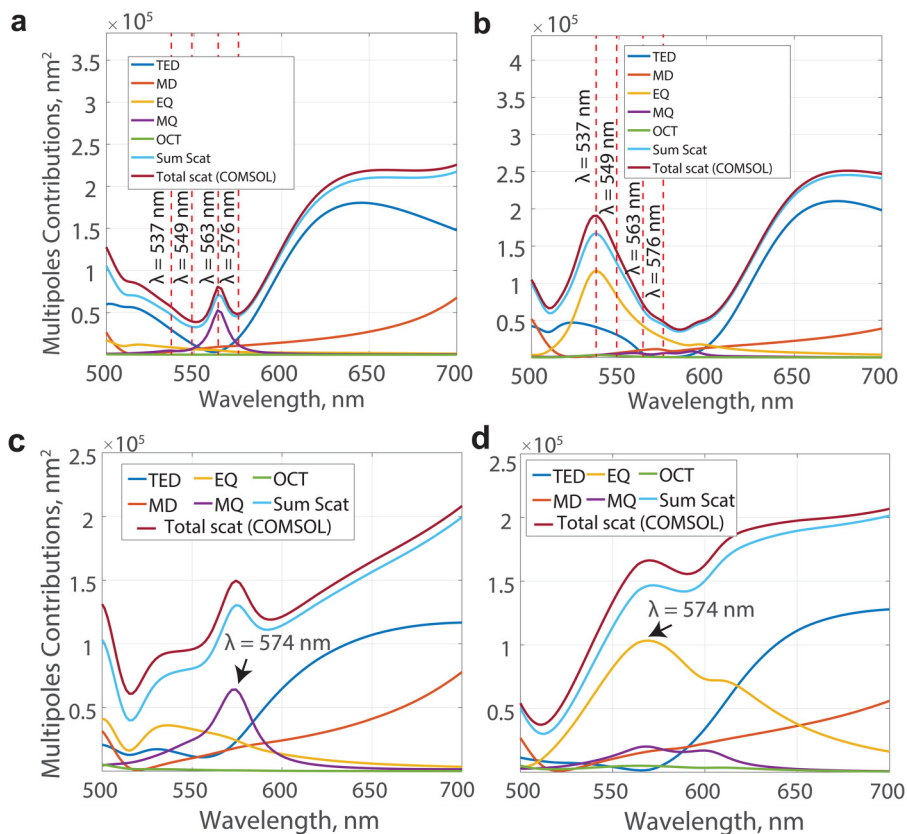


FIG. 2. Spectra of the scattering cross section and corresponding multipoles' contributions calculated for a silicon nanopyramid with height $H = 250 \text{ nm}$ and base edge $D = 250 \text{ nm}$ (a), (b) in air (c), (d) in medium with $n_{env} = 1.31$; electric field polarization of the incident plane wave is directed [(a), (c)] along the main axis of the nanopyramid [(b), (d)] perpendicular to the main axis of the nanopyramid. "Sum Scat" states for the scattering cross section as the sum of the multipole contributions; "Total scat (COMSOL)" states for the total scattering cross sections calculated directly in COMSOL.

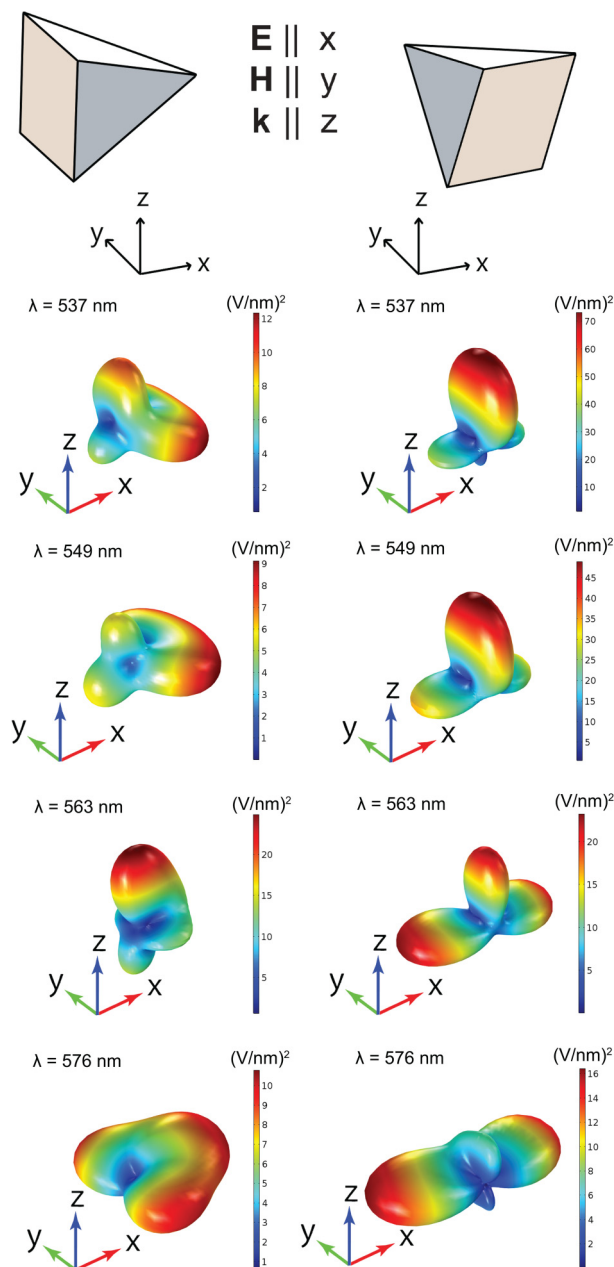


FIG. 3. Radiation patterns of the pyramidal nanoparticle with height $H = 250$ nm and base edge $D = 250$ nm at the indicated wavelengths. Left column corresponds to the electric field polarization of the incident plane wave directed along the main axis of the nanoparticle; right column corresponds to the polarization perpendicular to the main axis.

perpendicular polarization. Far-field radiation patterns have been drawn in COMSOL Multiphysics package.

For $\lambda = 537$ nm in the right column of Fig. 3, we show the far-field radiation pattern corresponding to the resonant excitation

of the EQ moment [Fig. 2(b)]. Such a dominating contribution of EQ provides four scattering lobes; side-scattering in this case directed along the polarization of the electric field. Noticeable contribution of TED moment breaks the symmetry of the forward and backward scattering. For $\lambda = 549$ nm, the relative EQ contribution decreases, and in the right side of Fig. 3, we note the suppression of the backward scattering in comparison with the previous case. For the opposite polarization of the incident wave (left column in Fig. 3), the combination of several multipoles' contributions leads to dominating side-scattering in a selected direction together with two weaker radiation lobes.

As λ increases to 563 nm, one can note the resonant excitation of MQ moment in Fig. 2(a). It leads to the corresponding far-field radiation pattern, depicted in the left column in Fig. 3; For the polarization perpendicular to the main axis of the pyramid, radiation pattern tends to provide dominating side-scattering due to the mutual interaction between multipoles. Thereby, we note the suppression of the forward and backward scattering with simultaneous amplification of side-scattering in the same direction with respect to the pyramid location.

Interestingly, side-scattering prevails for both polarization cases at $\lambda = 576$ nm. As shown in the left side of Fig. 3, the mutual interaction between TED, MD, and MQ moments [Fig. 2(a)] provides unusual side-scattering in three directions. However, it can be switched to the side-scattering along the electric field polarization of the incident wave, as depicted in the right column of Fig. 3. Thus, such pyramids can be used to change the far-field scattering in the particular direction by changing the incident wave polarization. We note that polarization change leads to the scattering suppression toward the apex of the nanoparticle. It is important that the nanoparticle scatters light in a plane, perpendicular to the k -vector of the incident wave. Another approach to control the light scattering in this plane is rotating the nanoparticle around the incident wave k -vector.

Let us now consider the case of dielectric medium, which is more interesting for potential experimental verification. We show that surrounding medium with $n_{env} = 1.31$ allows switching between resonant excitations of MQ and EQ moments. To confirm this effect in Fig. 4, we show 2D and 3D far-field radiation patterns at $\lambda = 574$ nm. Figures 4(a) and 4(b) present 3D and 2D radiation patterns for the incident wave polarization directed along the main axis of a nanoparticle. The blue line in Fig. 4(b) shows the distinctive MQ radiation pattern with 4-lobes in the plane of magnetic field polarization. In turn, the green line in Fig. 4(d) shows the distinctive radiation pattern with 4-lobes in the plane of electric field polarization. While comparing spectra in Figs. 2(c) and 2(d), one can see that EQ resonant excitation [Fig. 2(d)] is stronger than MQ resonant excitation [Fig. 2(c)]; it explains more symmetrical quadrupole radiation pattern in Fig. 4(d). However, additional contributions of another multipole moments [Figs. 2(c) and 2(d)] affect far-field radiation as well. It can be seen in Fig. 4(b) (green line) and in Fig. 4(d) (blue line). Thus, the simple change of polarization conditions for silicon nanoparticle in the dielectric medium allows switching between EQ and MQ resonant excitation and provide corresponding changes in far-field radiation patterns. However, side-scattering lobes do not change the direction with respect to the pyramid

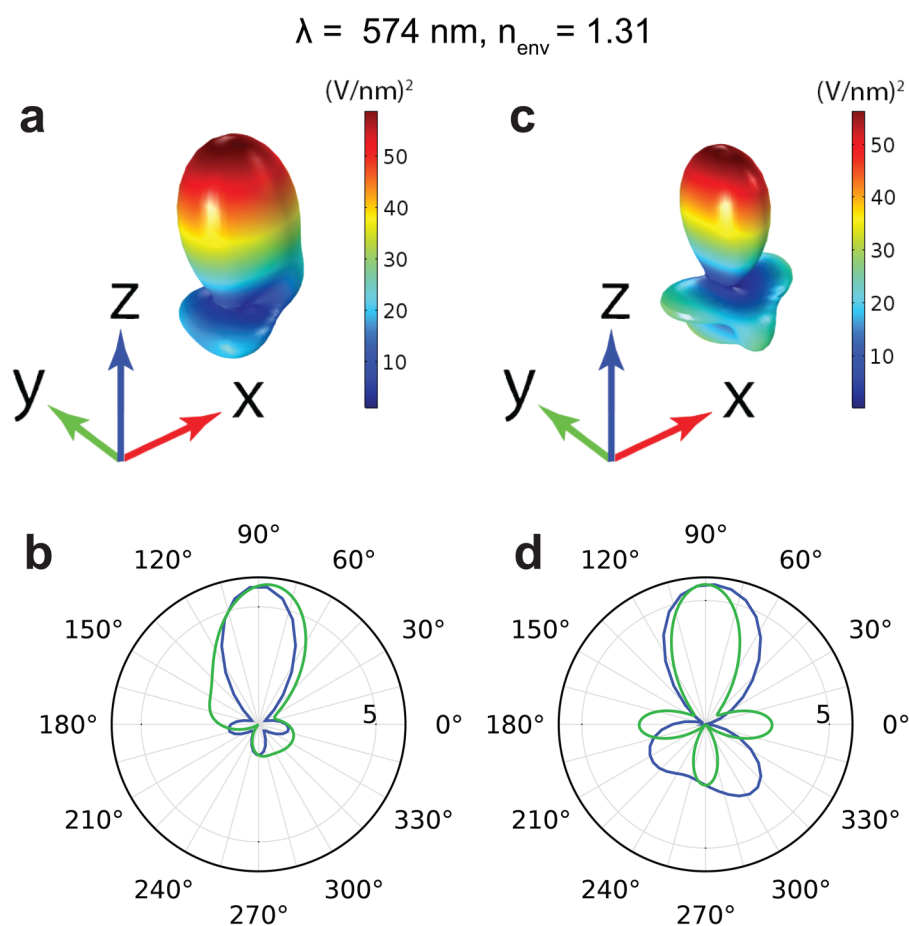


FIG. 4. 3D and 2D radiation patterns of the pyramidal nanoparticle in the medium with $n_{\text{env}} = 1.31$ at wavelength $\lambda = 574 \text{ nm}$. Electric field polarization of the incident plane wave directed [(a), (b)] along the symmetry axis of the pyramid (x axis). In (c) and (d), the incident electric field is directed along the y axis perpendicular to the symmetry axis (x axis). Green lines in (b) and (d) correspond to the plane of electric field polarization; blue lines correspond to the plane of magnetic field polarization. In both cases, the external wave propagates along the z axis.

location [the coordinate system in Figs. 4(a) and 4(b) is tied to the incident wave as well as in Fig. 3].

To underline the difference between EQ and MQ resonant excitation, in Fig. 5, we present the electric field concentration inside the pyramid. The coordinate system shows the incident wave polarization. One can note that MQ resonance leads to a stronger electric field concentration. The shape of a distribution also differs for the different incident wave polarizations. Thus, pyramidal

nanoparticles can be used not only to switch far-field radiation patterns but also to manipulate electric field concentration inside nanoobjects. Fabrication of such asymmetric structures can be done, for example, using the additive nanomanufacturing.⁴³ Additional discussion on the fabrication of pyramidal structures at the nanoscale can be found, for instance, in Refs. 44 and 45. Insights from this study can be used to control light direction by the incident wave polarization in optical switches and filters.

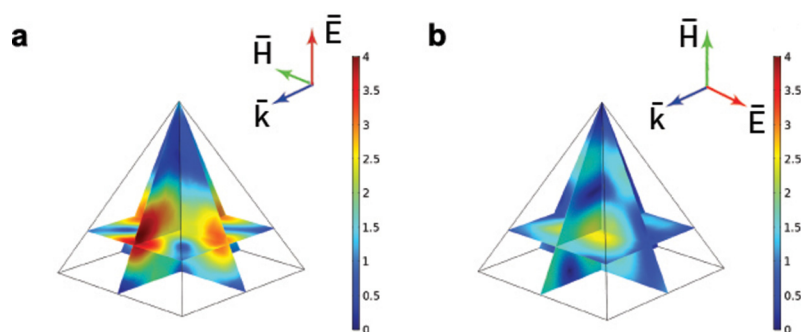


FIG. 5. Electric field distribution and concentration inside the silicon nanopyramid due to resonant excitation of (a) MQ (b) EQ moment. Electric field polarization of the incident plane wave directed (a) along the main axis of the pyramid and (b) perpendicular to the main axis.

IV. CONCLUSION

In conclusion, we utilize the multipole decomposition approach to explore the dependence of scattering by the silicon nanopillar on the polarization of the incident wave. Our study covers scattering properties of the nanopillars in air and lossless dielectric media with $n_{\text{env}} = 1.31$ in the visible range. It has been demonstrated that such particles allow switching between resonant excitations of EQ and MQ moments. Such switching crucially changes far-field scattering by the considered nanoparticles. Moreover, it is possible to switch the direction of the side-scattering in particular wavelength by changing the polarization of the incident wave. It is also possible to control light scattering by rotating the nanopillar around the incident wave k -vector.

We show that using the influence of the surrounding medium, it is possible to resonantly excite either EQ or MQ multipole moment depending on the polarization conditions. Such switching not only changes the far-field scattering but also provides significant changes in the electric field distribution and concentration inside the particle. Worth noting that for smaller nanopillars, similar effects are expected to appear at the smaller wavelengths due to Maxwell equations' scaling. In the considered spectral range, small pillars will scatter light due to the excitation of low-order multipoles (electric and magnetic dipole moments). Our study provides important information that can be used in the development of optical antennas, switches, and polarization filters at the nanoscale.

ACKNOWLEDGMENTS

The authors thank Svetlana Korinskaya for help with the artistic work. This work has been supported by the Israel Innovation Authority-Kamin Program (Grant No. 62045). A.S.S. acknowledges the support of the Russian Fund for Basic Research within the projects 18-02-00414, 18-52-00005, and the support of the Ministry of Education and Science of the Russian Federation (GOSZADANIE Grant No. 3.4982.2017/6.7). The development of the analytical approach and the calculations of multipole moments have been partially supported by the Russian Science Foundation (Grant No. 16-12-10287). Support has been provided by the Government of the Russian Federation (Grant No. 08-08). The research described was performed by Pavel Terekhov as a part of the joint Ph.D. program between the BGU and ITMO. The work was partially supported by the Deutsche Forschungsgemeinschaft (DFG) (German Research Foundation) under Germany's Excellence Strategy within the Cluster of Excellence PhoenixD (EXC 2122, Project ID 390833453).

REFERENCES

- ¹A. Karabchevsky, A. Mosayyebi, and A. V. Kavokin, "Tuning the chemiluminescence of a luminol flow using plasmonic nanoparticles," *Light Sci. Appl.* **5**, e16164 (2016).
- ²A. Karabchevsky, J. S. Wilkinson, and M. N. Zervas, "Transmittance and surface intensity in 3d composite plasmonic waveguides," *Opt. Express* **23**, 14407–14423 (2015).
- ³A. B. Evlyukhin, C. Reinhardt, A. Seidel, B. S. Lukyanchuk, and B. N. Chichkov, "Optical response features of Si-nanoparticle arrays," *Phys. Rev. B* **82**, 045404 (2010).
- ⁴A. I. Kuznetsov, A. E. Miroshnichenko, Y. H. Fu, J. Zhang, and B. Lukyanchuk, "Magnetic light," *Sci. Rep.* **2**, 492 (2012).
- ⁵S. Jahani and Z. Jacob, "All-dielectric metamaterials," *Nat. Nanotechnol.* **11**, 23–36 (2016).
- ⁶E. Betzig and J. K. Trautman, "Near-field optics: Microscopy, spectroscopy, and surface modification beyond the diffraction limit," *Science* **257**, 189–195 (1992).
- ⁷D. K. Gramotnev and S. I. Bozhevolnyi, "Plasmonics beyond the diffraction limit," *Nat. Photonics* **4**, 83 (2010).
- ⁸A. B. Evlyukhin, S. M. Novikov, U. Zywietz, R. L. Eriksen, C. Reinhardt, S. I. Bozhevolnyi, and B. N. Chichkov, "Demonstration of magnetic dipole resonances of dielectric nanospheres in the visible region," *Nano Lett.* **12**, 3749–3755 (2012).
- ⁹A. Garcia-Etxarri, R. Gómez-Medina, L. S. Froufe-Perez, C. Lopez, L. Chantada, F. Scheffold, J. Aizpurua, M. Nieto-Vesperinas, and J. J. Sáenz, "Strong magnetic response of submicron silicon particles in the infrared," *Opt. Express* **19**, 4815–4826 (2011).
- ¹⁰Z.-J. Yang, R. Jiang, X. Zhuo, Y.-M. Xie, J. Wang, and H.-Q. Lin, "Dielectric nanoresonators for light manipulation," *Phys. Rep.* **701**, 1–50 (2017).
- ¹¹J. B. Khurgin, G. Sun, and R. Soref, "Practical limits of absorption enhancement near metal nanoparticles," *Appl. Phys. Lett.* **94**, 071103 (2009).
- ¹²J. D. Jackson, *Classical Electrodynamics* (AAPT, 1999).
- ¹³P. D. Terekhov, K. V. Baryshnikova, Y. A. Artemyev, A. Karabchevsky, A. S. Shalin, and A. B. Evlyukhin, "Multipolar response of nonspherical silicon nanoparticles in the visible and near-infrared spectral ranges," *Phys. Rev. B* **96**, 035443 (2017).
- ¹⁴P. D. Terekhov, K. V. Baryshnikova, A. S. Shalin, A. Karabchevsky, and A. B. Evlyukhin, "Resonant forward scattering of light by high-refractive-index dielectric nanoparticles with toroidal dipole contribution," *Opt. Lett.* **42**, 835–838 (2017).
- ¹⁵A. E. Krasnok, A. E. Miroshnichenko, P. A. Belov, and Y. S. Kivshar, "All-dielectric optical nanoantennas," *Opt. Express* **20**, 20599–20604 (2012).
- ¹⁶K. V. Baryshnikova, A. Novitsky, A. B. Evlyukhin, and A. S. Shalin, "Magnetic field concentration with coaxial silicon nanocylinders in the optical spectral range," *JOSA B* **34**, D36–D41 (2017).
- ¹⁷V. Kozlov, D. Filonov, A. S. Shalin, B. Z. Steinberg, and P. Ginzburg, "Asymmetric backscattering from the hybrid magneto-electric meta particle," *Appl. Phys. Lett.* **109**, 203503 (2016).
- ¹⁸D. Markovich, K. Baryshnikova, A. Shalin, A. Samusev, A. Krasnok, P. Belov, and P. Ginzburg, "Enhancement of artificial magnetism via resonant bianisotropy," *Sci. Rep.* **6**, 22546 (2016).
- ¹⁹A. Katiyi and A. Karabchevsky, "Figure of merit of all-dielectric waveguide structures for absorption overtone spectroscopy," *J. Lightwave Technol.* **35**, 2902–2908 (2017).
- ²⁰N. Bontempi, K. E. Chong, H. W. Orton, I. Staude, D.-Y. Choi, I. Alessandri, Y. S. Kivshar, and D. N. Neshev, "Highly sensitive biosensors based on all-dielectric nanoresonators," *Nanoscale* **9**, 4972–4980 (2017).
- ²¹T. Wood, M. Naffouti, J. Berthelot, T. David, J.-B. Claude, L. Métayer, A. Delobbe, L. Favre, A. Ronda, I. Berbezier *et al.*, "All-dielectric color filters using SiGe-based Mie resonator arrays," *ACS Photonics* **4**, 873–883 (2017).
- ²²C.-Y. Yang, J.-H. Yang, Z.-Y. Yang, Z.-X. Zhou, M.-G. Sun, V. E. Babicheva, and K.-P. Chen, "Nonradiating silicon nanoantenna metasurfaces as narrowband absorbers," *ACS Photonics* **5**, 2596–2601 (2018).
- ²³P. D. Terekhov, K. V. Baryshnikova, Y. Greenberg, Y. H. Fu, A. B. Evlyukhin, A. S. Shalin, and A. Karabchevsky, "Enhanced absorption in all-dielectric metasurfaces due to magnetic dipole excitation," *Sci. Rep.* **9**, 3438 (2019).
- ²⁴Y. Galutin, E. Falek, and A. Karabchevsky, "Invisibility cloaking scheme by evanescent fields distortion on composite plasmonic waveguides with Si nanospacer," *Sci. Rep.* **7**, 12076 (2017).
- ²⁵P. D. Terekhov, V. E. Babicheva, K. V. Baryshnikova, A. S. Shalin, A. Karabchevsky, and A. B. Evlyukhin, "Multipole analysis of dielectric metasurfaces composed of non-spherical nanoparticles and lattice invisibility effect," *Phys. Rev. B* **99**, 045424 (2019).
- ²⁶K. V. Baryshnikova, D. A. Smirnova, B. S. Lukyanchuk, and Y. S. Kivshar, "Optical anapoles: Concepts and applications," *Adv. Opt. Mater.* 1801350 (published online).

- ²⁷A. E. Miroshnichenko, A. B. Evlyukhin, Y. F. Yu, R. M. Bakker, A. Chipouline, A. I. Kuznetsov, B. Luk'yanchuk, B. N. Chichkov, and Y. S. Kivshar, "Nonradiating anapole modes in dielectric nanoparticles," *Nat. Commun.* **6**, 8069 (2015).
- ²⁸K. Baryshnikova, D. Filonov, C. Simovski, A. Evlyukhin, A. Kadochkin, E. Nenasheva, P. Ginzburg, and A. S. Shalin, "Giant magnetoelectric field separation via anapole-type states in high-index dielectric structures," *Phys. Rev. B* **98**, 165419 (2018).
- ²⁹P. Terekhov, K. Baryshnikova, A. Evlyukhin, and A. Shalin, "Destructive interference between electric and toroidal dipole moments in TiO_2 cylinders and frustums with coaxial voids," *J. Phys. Conf. Ser.* **929**, 012065 (2017).
- ³⁰M. Balezin, K. V. Baryshnikova, P. Kapitanova, and A. B. Evlyukhin, "Electromagnetic properties of the great pyramid: First multipole resonances and energy concentration," *J. Appl. Phys.* **124**, 034903 (2018).
- ³¹I. Staude and J. Schilling, "Metamaterial-inspired silicon nanophotonics," *Nat. Photonics* **11**, 274 (2017).
- ³²D. G. Baranov, D. A. Zuev, S. I. Lepeshov, O. V. Kotov, A. E. Krasnok, A. B. Evlyukhin, and B. N. Chichkov, "All-dielectric nanophotonics: The quest for better materials and fabrication techniques," *Optica* **4**, 814–825 (2017).
- ³³A. I. Kuznetsov, A. E. Miroshnichenko, M. L. Brongersma, Y. S. Kivshar, and B. Luk'yanchuk, "Optically resonant dielectric nanostructures," *Science* **354**, aag2472 (2016).
- ³⁴E. D. Palik, *Handbook of Optical Constants of Solids* (Academic Press, 1998), Vol. 3.
- ³⁵A. B. Evlyukhin, T. Fischer, C. Reinhardt, and B. N. Chichkov, "Optical theorem and multipole scattering of light by arbitrary shaped nanoparticles," *Phys. Rev. B* **94**, 205434 (2016).
- ³⁶R. Alaei, C. Rockstuhl, and I. Fernandez-Corbaton, "An electromagnetic multipole expansion beyond the long-wavelength approximation," *Opt. Commun.* **407**, 17–21 (2018).
- ³⁷M. I. Tribelsky, J.-M. Geffrin, A. Litman, C. Eyraud, and F. Moreno, "Small dielectric spheres with high refractive index as new multifunctional elements for optical devices," *Sci. Rep.* **5**, 12288 (2015).
- ³⁸R. E. Raab and O. L. De Lange, *Multipole Theory in Electromagnetism* (Oxford University, Clarendon, Oxford, 2005).
- ³⁹D. W. Pepper and J. C. Heinrich, *The Finite Element Method: Basic Concepts and Applications with MATLAB, MAPLE, and COMSOL* (CRC Press, 2017).
- ⁴⁰See www.comsol.com for more information about COMSOL Multiphysics.
- ⁴¹P. D. Terekhov, H. K. Shamkhi, E. A. Gurvitz, K. V. Baryshnikova, A. B. Evlyukhin, A. S. Shalin, and A. Karabchevsky, "Broadband forward scattering from dielectric cubic nanoantenna in lossless media," *Opt. Express* **27**, 10924–10935 (2019).
- ⁴²E. A. Gurvitz, K. S. Ladutenko, P. A. Dergachev, A. B. Evlyukhin, A. Miroshnichenko, and A. S. Shalin, "The high-order toroidal moments and anapole states in all-dielectric photonics," *Laser Photo. Rev.* (published online).
- ⁴³D. S. Engstrom, B. Porter, M. Pacios, and H. Bhaskaran, "Additive nanomanufacturing—A review," *J. Mater. Res.* **29**, 1792–1816 (2014).
- ⁴⁴J. T. Sheu, S. Yeh, C. Wu, and K. You, "Fabrication of ultrahigh-density nanopillar arrays (NPAS) on (100) silicon wafer using scanning probe lithography and anisotropic wet etching," in *Proceedings of the 2nd IEEE Conference on Nanotechnology* (IEEE, 2002), pp. 277–281.
- ⁴⁵Y.-C. Lien, Y.-H. Pai, and G.-R. Lin, "Si nano-dots and nano-pyramids dependent light emission and charge accumulation in ITO/ SiO_x /p-si MOS diode," *IEEE J. Quantum Electron.* **46**, 121–127 (2010).